Proceedings of IMECE2006
2006 ASME International Mechanical Engineering Congress and Exposition
November 5-10, 2006, Chicago, Illinois, USA

IMECE2006-14646

AN ACTUATION MECHANISM FOR A DUAL-ARM ROBOTIC MANIPULATOR

Martin Hosek

Brooks Automation, Inc.
16 Elizabeth Drive
Chelmsford, MA 01824
martin.hosek@brooks.com

ABSTRACT

An actuation mechanism for a dual-arm scara-type robot for automated pick-place operations in semiconductor and flat-panel-display manufacturing applications is described. The mechanism consists of a pivoting platform and two linkages coupled to the platform through a pair of revolute joints. The opposite ends of the linkages are connected to the upper arms of the robot by another pair of revolute joints, forming a pair of three-bar mechanisms coupled through the pivoting platform. When the platform is in its neutral position, both of the arms are retracted. The geometry of the components of the mechanism is selected so that rotation of the platform from the neutral position in one direction produces desirable radial motion of one arm while the other arm is kept almost stationary in the retracted position. The arms exchange their roles when the platform rotates from the neutral position in the opposite direction. Alternatively, to achieve absolutely no motion of the retracted arm while the other one extends, the pivoting motion of the platform can be replaced by a rocking arrangement with two pivot points. In this configuration, the locations of the two pivot points coincide with the locations of the revolute joints between the linkages and the upper arms when the platform is in the neutral position. As a result, rotation of the platform with respect to one of the pivot points produces no motion of the corresponding arm while the other one extends. Compared to a conventional design, which utilizes a pair of motors coupled to the robot arms through a pair of belt arrangements, the present mechanism eliminates one of the two motors, including its electronic circuitry, and replaces the belt drives with rigid linkages, thus reducing the complexity and cost, and improving the reliability and cleanliness of the robotic system.

1 INTRODUCTION

The existing manufacturing technologies for semiconductor integrated circuits (IC) and flat panel displays (FPD) include processing of silicon wafers and glass panels, referred to as substrates, in fully automated cluster tools (Beaulieu and Pippins 1999, Almogy 2001, Garriga 2002). A typical cluster tool (Figure 1) consists of a circular vacuum chamber with load locks and process modules connected radially to the circumference of the chamber in a star pattern. The tool is serviced by a robot (Davis and Brooks 1988, Shiraiwa 1995, Caveney and Hofmeister 1998) which is located at the center of the chamber, and cycles the substrates from the load locks through the process modules and back to the load locks. Another robot is located in an atmospheric transfer module which serves as an interface between the load locks of the vacuum chamber and standardized load ports serviced by an external transportation system.

Typical operations performed by the robots include elementary rotational and radial straight-line moves (Lucas 1997, Hosek and Elmali 2001), which are often combined and blended into more complicated planar or three-dimensional trajectories in order to comply with complex workspace geometries (Hosek and Elmali 2002, 2003). In many applications, a cluster tool robot is required to replace a processed substrate with a fresh substrate. This operation, referred to as a substrate exchange, often directly affects the throughput performance of the cluster tool, i.e., the number of substrates processed by the tool per hour. In order to complete a substrate exchange operation, a single-end-effector robot picks the processed substrate from the workstation, places it to a specified location, picks a fresh substrate from another location, and places it to the workstation. This sequence typically requires a total of thirteen discrete moves. The number of moves, and thus the substrate exchange time, can be improved substantially by utilizing a robot with two end-effectors (Hendrickson 1993, Davis and Hofmeister 1997, Hosek and Valasek 2003). In this case, the robot picks the processed substrate by one end-effector and replaces it by a fresh substrate readily available on the other end-effector, thus reducing

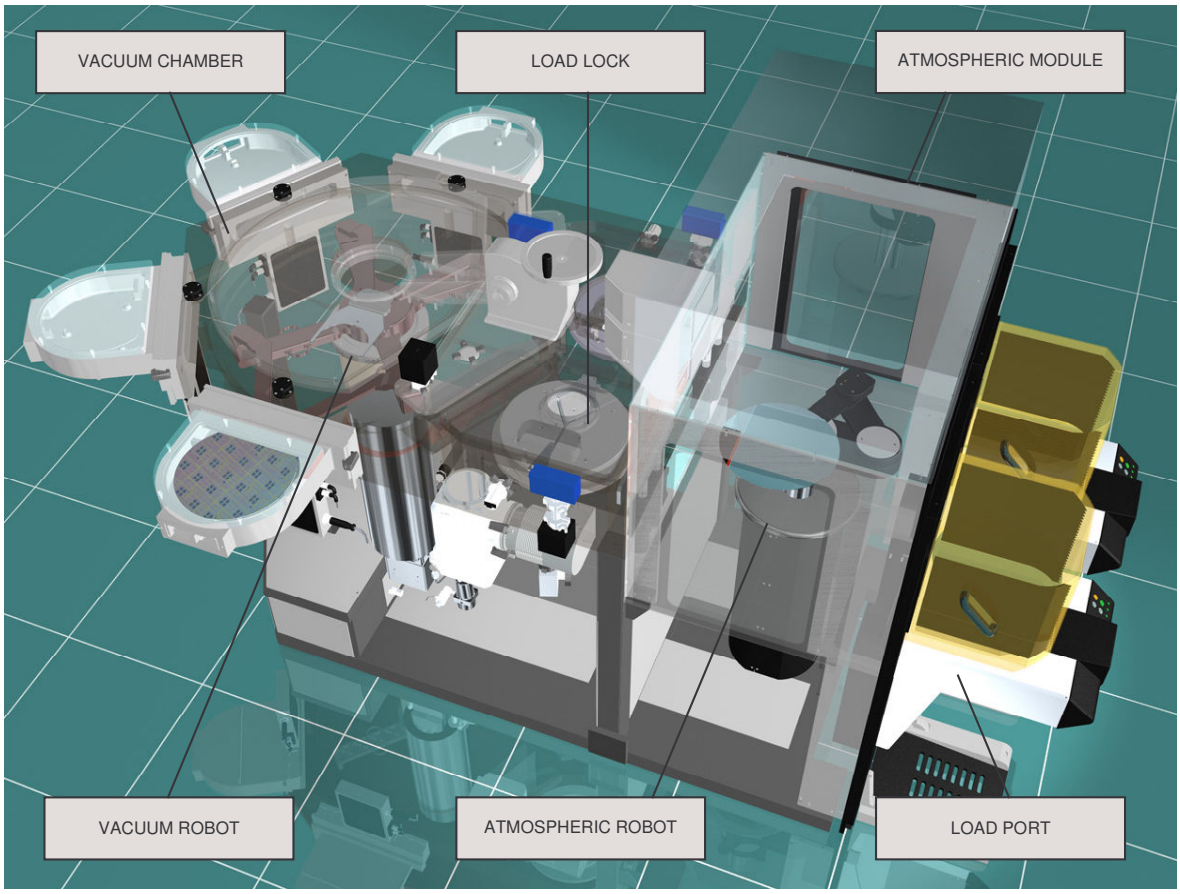

Figure 1: Cluster tool platform for semiconductor manufacturing applications.

substantially the number of moves on the critical path (Hosek 2003).

Among various dual-end-effector robot design configurations, dual-arm scara-type robots belong to particularly popular solutions, both for vacuum and atmospheric applications. A typical dual-arm scara-type robot mechanism is schematically shown in Figure 2. It is built around a pivoting hub 1, which carries two arms, left and right. The left arm, also referred to as the left linkage, consists of the left upper arm 2L, left forearm 3L, and left end-effector 4L, coupled in series through revolute joints. A belt arrangement comprising the pulleys 5L, 6L and belt 7L is employed to constrain the motion of the linkage so that rotation of the upper arm 2L with respect to the hub 1 produces equal rotation of the forearm 3L in the opposite direction. This is achieved through a 2:1 ratio between the radii of the pulley 5L, connected to the hub 1, and the pulley 6L, attached to the forearm 3L. Another belt arrangement, which includes the pulleys 8L, 9L and belt 10L, is utilized to maintain radial orientation of the end-effector 4L. In this case, a 1:2 ratio between the radii of the pulleys 8L and 9L, coupled to the upper arm 2L and end-effector 4L, respectively, is used. The right arm, also referred to as the right linkage, is designed as a mirror image of the left one, comprising the right upper arm 2R, right forearm 3R, right end-effector 4R, pulleys 5R and 6R, belt 7R, pulleys 8R and 9R, and belt 10R. The two end-effectors, 4L and 4R, move in different horizontal planes to allow for unrestricted motion of the two linkages of the robot. By rotating the left and right upper arms 2L and 2R, the respective linkages can be extended independently in a common radial direction with respect to the pivoting point of the hub 1.

Conventionally, the robot arm is actuated by three motors, most often arranged in a coaxial manner, coupled to the mechanism through hollow shafts. While the most outer shaft is typically connected directly to the hub 1, the two inner shafts are coupled to the upper arms 2L and 2R through independent belt drives. In particular, the left upper arm 2L is driven by the pulley 11L and belt 12L, and the right upper arm 2R is actuated via the pulley 11R and belt 12R. The entire robot can be rotated with respect to the pivot point of the hub 1 by moving all of the drive shafts equally in the specified direction of rotation. The left linkage, which carries the end-effector 4L, can be extended radially with respect to the pivoting point of the hub 1 by rotating the corresponding drive shaft in the clockwise direction while the other two shafts are kept stationary. Similarly, the right linkage and end-effector 4R extend radially when the other inner drive shaft rotates in the counterclockwise direction.

A typical mode of operation of the dual-arm scara-type robot is illustrated in Figure 3. Diagram (a) shows the arm in

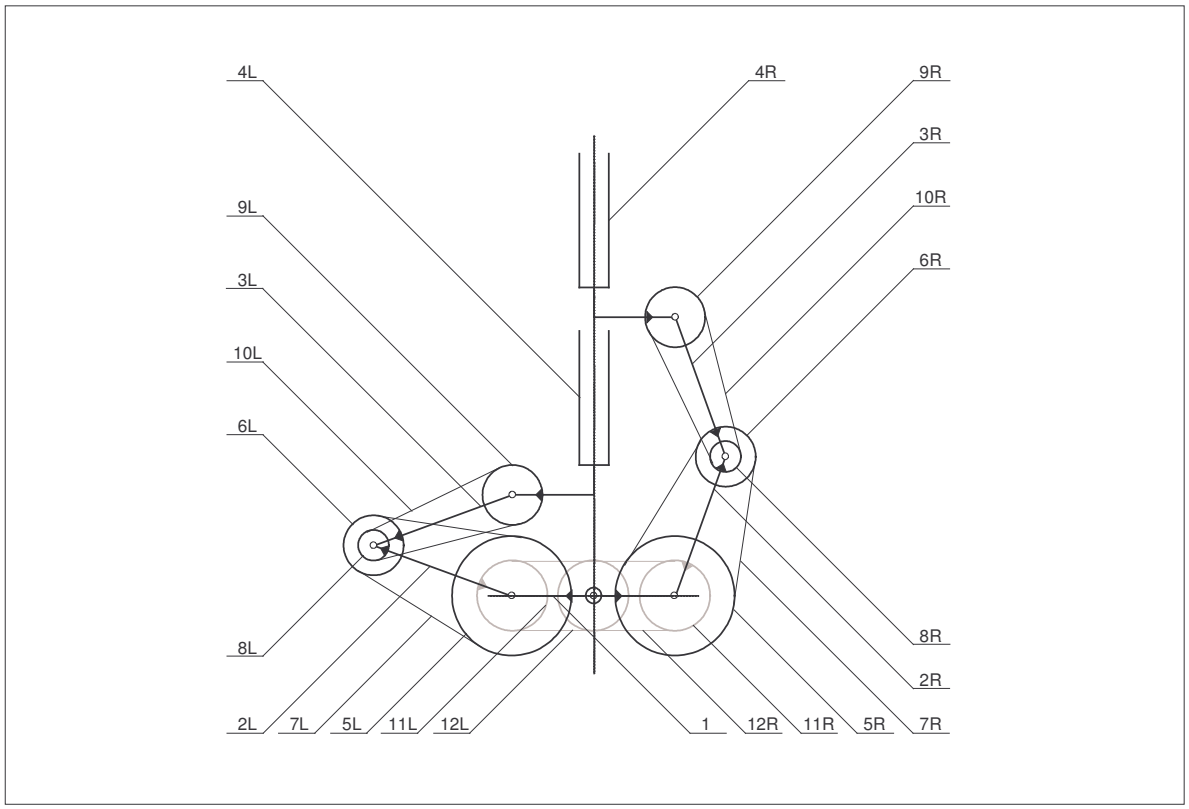

Figure 2: State-of-the art dual-arm scara-type robot.

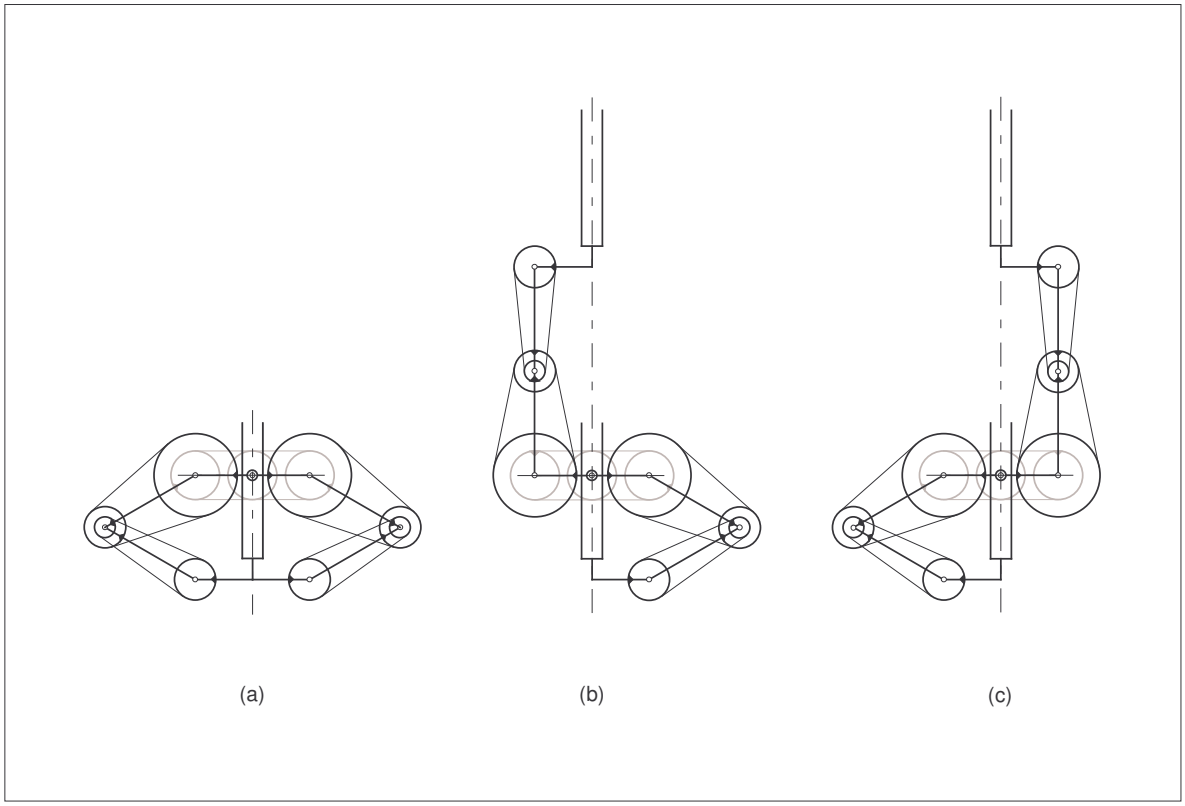

Figure 3: Typical operation of dual-arm scara-type robot, (a) both arms retracted, (b) left arm extended, (c) right arm extended.

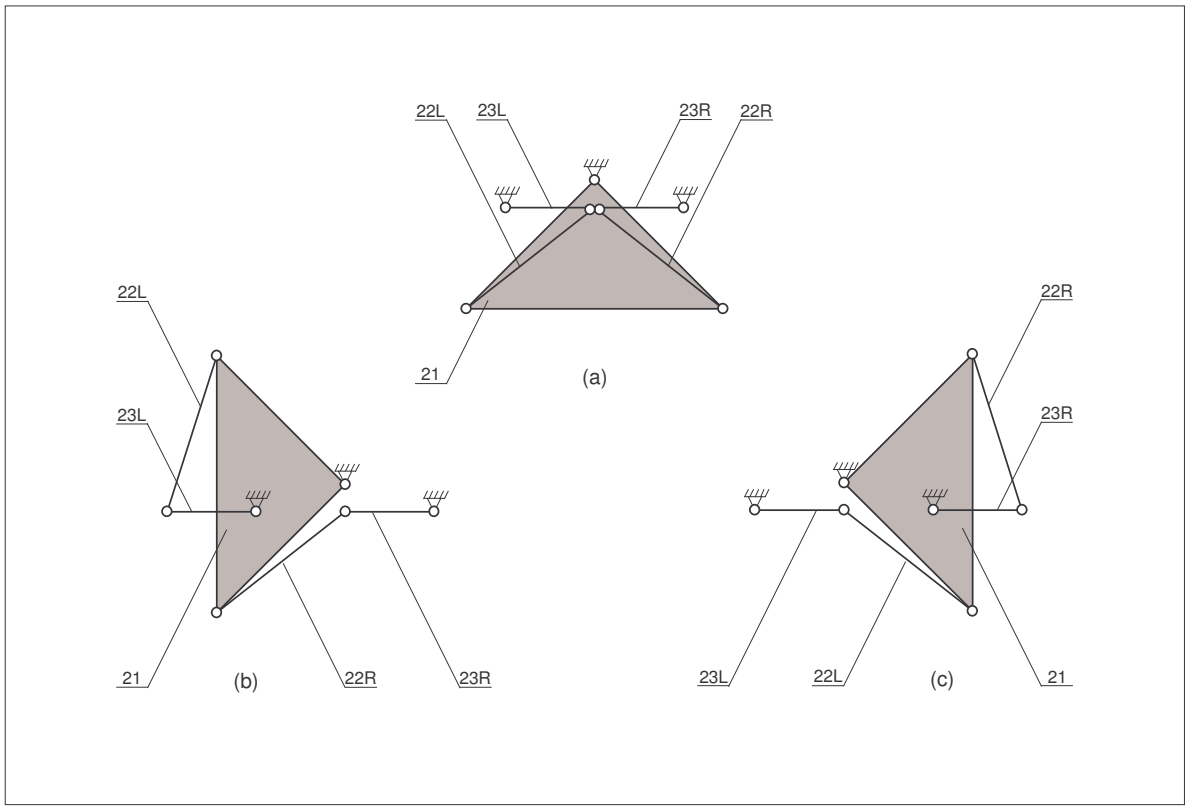

Figure 4: Pivoting actuation mechanism, (a) neutral position, (b) actuation of link 23L, (c) actuation of link 23R.

the retracted position with one end-effector above the other. In this case, both linkages are folded to minimize the area required to rotate the arm. In a standard substrate exchange sequence, an empty linkage extends radially from the retracted position to a workstation, as indicated in diagram (b), picks a processed substrate, and retracts back to the folded position of diagram (a). In the next step, the vertical position of the arm is adjusted for the other linkage to be able to enter the workstation. Once the vertical position has been adjusted, the other linkage, which carries a fresh substrate, extends radially to the workstation, as depicted in diagram (c), places the substrate, and returns to the retracted position shown in diagram (a). Note that the two linkages never move simultaneously, i.e., one linkage is always kept stationary while the other one extends and retracts.

In this paper, a new actuation scheme for the dual-arm scara-type robot is presented which utilizes a single motor to control the radial motion of both arms of the robot. The motor drives a pivoting platform with two links connected to the upper arms of the robot, forming a pair of three-bar mechanisms coupled through the pivoting platform. When the platform is in its neutral position, both of the arms of the robot are retracted. The geometry of the actuation mechanism is selected so that rotation of the platform from the neutral position in one direction produces desirable radial motion of one arm while the other arm is kept almost stationary in the retracted position. The arms exchange their roles when the platform rotates from the neutral position in the opposite direction. Alternatively, to achieve zero motion of the retracted arm while the other one is extending, the pivoting motion of the platform can be replaced by a rocking arrangement with two pivot points. Compared to the conventional design, which utilizes a pair of motors coupled to the robot arms through a pair of belt arrangements, the proposed mechanisms eliminate one of the two motors, including its electronic circuitry, and replace the belt drives with rigid linkages, thus reducing the complexity and cost, and improving the reliability and cleanliness of the robotic system.

The document is structured as follows: the pivoting actuation mechanism for the dual-arm scara-type robot is described in Section 2; the rocking version of the actuation mechanism is presented in Section 3; design considerations are discussed in Section 4; alternative kinematic configurations which provide equivalent or similar functionality are discussed in Section 5; the proposed actuation scheme is summarized briefly in Section 6.

2 PIVOTING ACTUATION MECHANISM

The pivoting actuation mechanism for the dual-arm scara-type robot of Section 1 is depicted schematically in Figure 4. The mechanism consists of a pivoting platform 21 and two linkages 22L, 22R, coupled to the platform 21 through a pair of revolute joints. The opposite ends of the linkages 22L and 22R are connected to additional two pivotable links 23L and 23R by another pair of revolute joints, forming a pair of three-bar

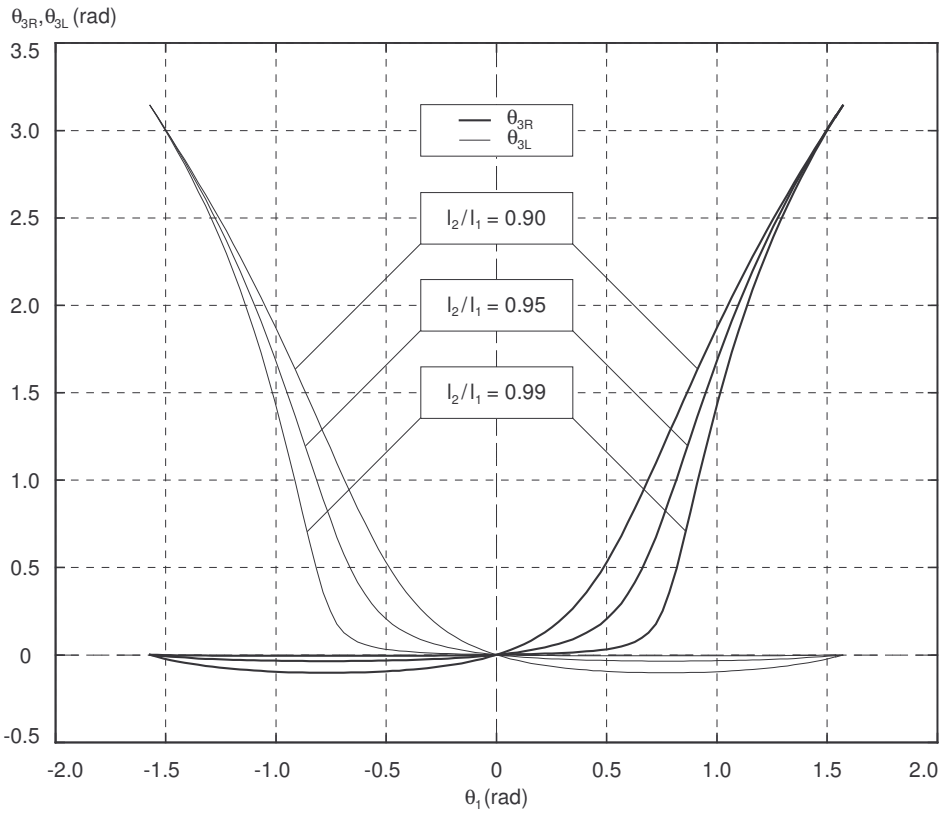

Figure 5: Kinematics of pivoting actuation mechanism.

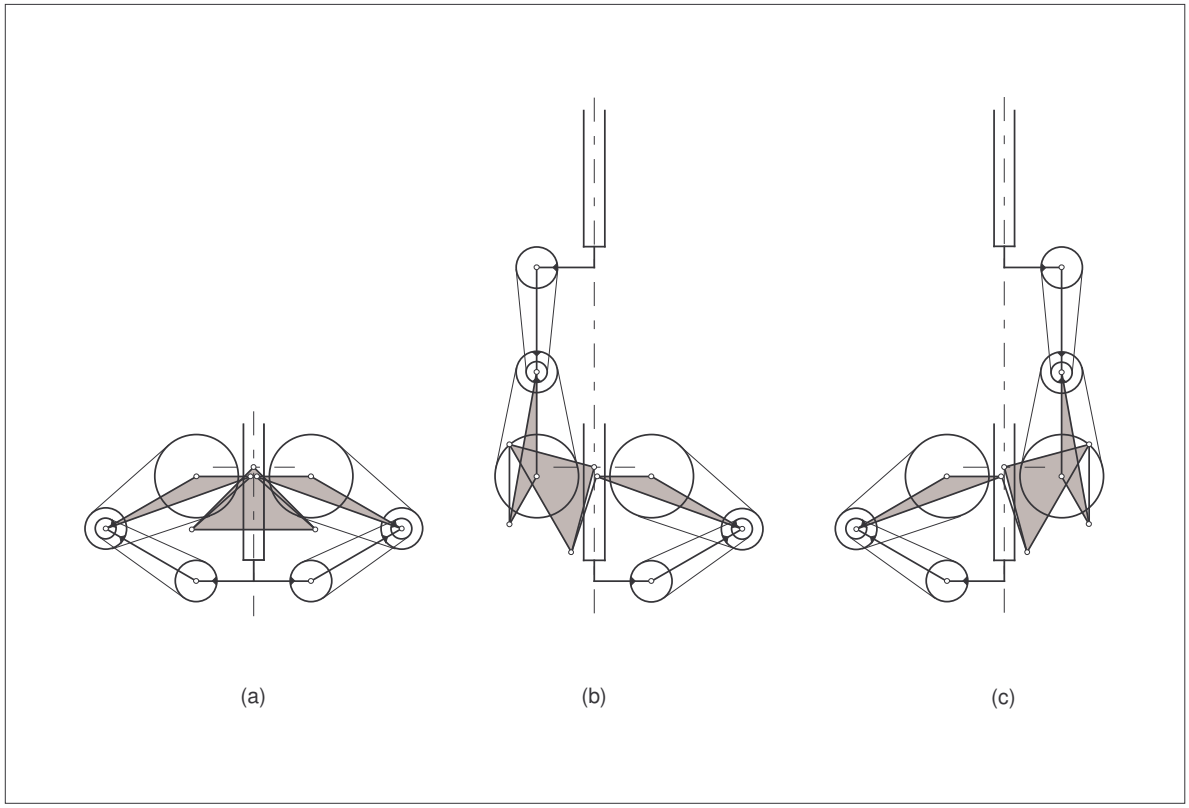

Figure 6: Dual-arm scara-type robot with pivoting mechanism, (a) both arms retracted, (b) left arm extended, (c) right arm extended.

mechanisms coupled through the pivoting platform 21. When the platform is in the neutral position of diagram (a), the links 23L and 23R are considered to be in their initial positions. The geometry of the components 21, 22L, 22R, 23L and 23R is selected so that rotation of the platform 21 from the neutral position in the clockwise direction produces desirable change of the angular orientation of the link 23L while the link 23R is kept almost stationary in the initial position, as indicated in diagram (b). In this particular case, the mechanism is designed so that 90-deg rotation of the platform 21 results in 180-deg motion of the link 23L. The links 23L and 23R exchange their roles when the platform 21 rotates from the neutral position in the counterclockwise direction, as shown in diagram (c).

The angular orientations of the links 23L and 23R as functions of the angular position of the platform 21 are graphed in Figure 5, where θ_1 denotes angular position of the platform 21, and θ_{3L} and θ_{3R} are angular orientations of the links 23L and 23R, respectively. The angles θ_1, θ_{3L} and θ_{3R} are measured with respect to the initial configuration of diagram (a) of Figure 4, with θ_1 and θ_{3R} being positive in the counterclockwise direction, and θ_{3L} being positive in the clockwise direction. Again, in accordance with Figure 4, the mechanism is designed so that 90-deg rotation of the platform 21 produces 180-deg motion of the link subject to actuation. However, a different range of motion can be achieved by selecting the dimensions of the mechanism accordingly, as explained in Section 4. The amount of the residual motion by the stationary link, 23R or 23L, while the other link, 23L or 23R, moves can be controlled by the ratio of l_2 over l_1, where l_1 stands for the distance between the pivoting point of the platform 21 and the revolute joints which couple the links 22L and 22R to the platform 21, and l_2 denotes the length of the links 22L and 22R. As indicated in Figure 5, the amount of the residual motion reduces as the ratio l_2/l_1 approaches the value of 1. However, the reduction of the residual motion of the stationary link, 23R or 23L, is achieved at the cost of increased nonlinearity of motion of the actuated link, 23L or 23R.

In Figure 6, the pivoting actuation mechanism of Figure 4 is applied to the dual-arm scara-type robot of Figure 2. In this case, the upper arms of the robot, 2L and 2R, assume the roles of the links 23L and 23R, respectively. When the platform 21 is in its neutral position, both of the arms of the robot are retracted, as indicated in diagram (a). As the platform 21 rotates clockwise, the left arm of the robot extends radially with respect to the pivot point of the platform 21 while the right arm remains almost stationary in its retracted position, as depicted in diagram (b). The two arms of the robot exchange their roles when the platform 21 rotates from the neutral position in the counterclockwise direction, as shown in diagram (c).

Note that the proposed mechanism does not increase the mechanical complexity of the robot arm since the pivoting platform 21 and the links 22L, 22R replace a pair of belt drives, each of them comprising two pulleys, a belt and a belt tensioner. Furthermore, since belt drives are typically associated with particle-generation and reliability-related problems, the proposed actuation mechanism represents a cleaner and more reliable solution. Finally, the overall complexity of the robot decreases substantially since the radial motion of the two arms is controlled by a single motor, thus eliminating completely one of the motors and its electronic circuitry, and further improving the reliability and cost aspects of the system.

3 ROCKING ACTUATION MECHANISM

Alternatively, to achieve zero motion of the retracted arm while the other one is extending, the pivoting motion of the platform can be replaced by a rocking arrangement with two pivot points. In this configuration, the locations of the two pivot points coincide with the locations of the revolute joints between the links of the mechanism and the upper arms of the robot when the platform is in the neutral position. As a result, rotation of the platform with respect to one of the pivot points produces no motion of the corresponding arm while the other one extends. An example configuration of such a mechanism is described below.

In Figure 7, diagram (a) shows schematically a platform 31 with a pair of links 30R and 30L hinged to the platform 31 at points A and B, respectively. The length of the links 30L and 30R is equal to the distance between points A and B. The free ends of the links 30L and 30R will be connected pivotably to stationary points C and D, respectively. The distance between points C and D is equal to the length of the links 30L and 30R. Keeping the orientation of the platform 31 constant, point A will coincide with point C, and point B will coincide with point D, as shown in diagram (b).

When torque is applied to the platform 31 in the counterclockwise direction, the platform 31 will rotate with respect to point D, as indicated in diagram (c). Similarly, applying torque in the clockwise direction yields rotation with respect to point C, as illustrated by diagram (d). This rocking motion is the key feature of the actuation mechanism. Note that the links 30L and 30R can be replaced conveniently by a set of pre-tensioned steel bands, a proven technology in precision robotic manipulators.

The platform 31 is then extended to carry an additional revolute joint E, as shown in diagram (e). A pair of links 32L and 32R are connected to the platform 31 at joint E. The lengths of the links 32L and 32R are equal to the distances AE and BE, respectively. The free ends F and G of the links 32L and 32R are coupled to another pair of links 33L and 33R which rotate with respect to points H and I. The dimensions and points of suspension are selected in such a manner that the trajectories of joints F and G pass through points C and D, respectively. The resulting mechanism is depicted in diagram (f).

The mechanism is shown again in its neutral position in diagram (a) of Figure 8. The links 30L and 30R are not depicted in this figure for the sake of simplicity. Instead, the pivot points for the clockwise and counterclockwise motion of the platform 31 are indicated as P_{CW} and P_{CC}, respectively. When torque is applied in the counterclockwise direction to the platform 31, the link 33L rotates, while the link 33R stays in the initial position, as indicated in diagrams (b) and (c). Similarly, when clockwise

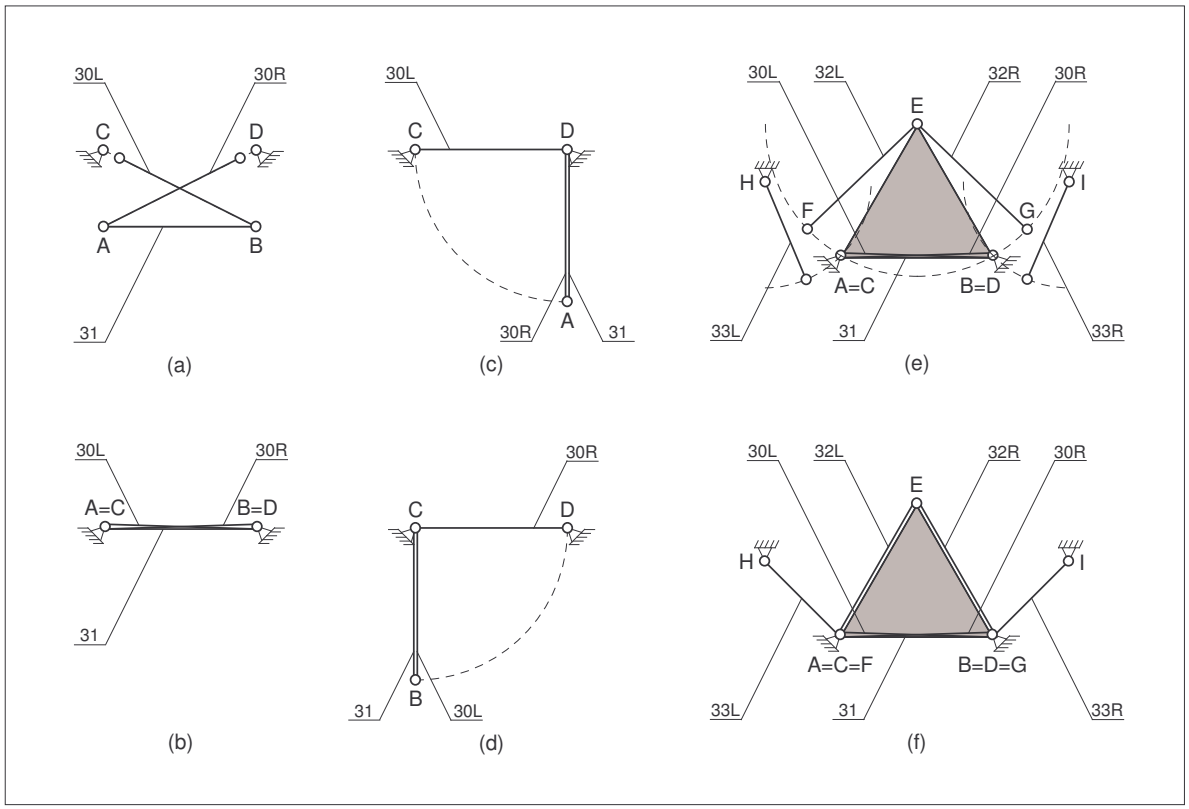

Figure 7: Construction of rocking actuation mechanism.

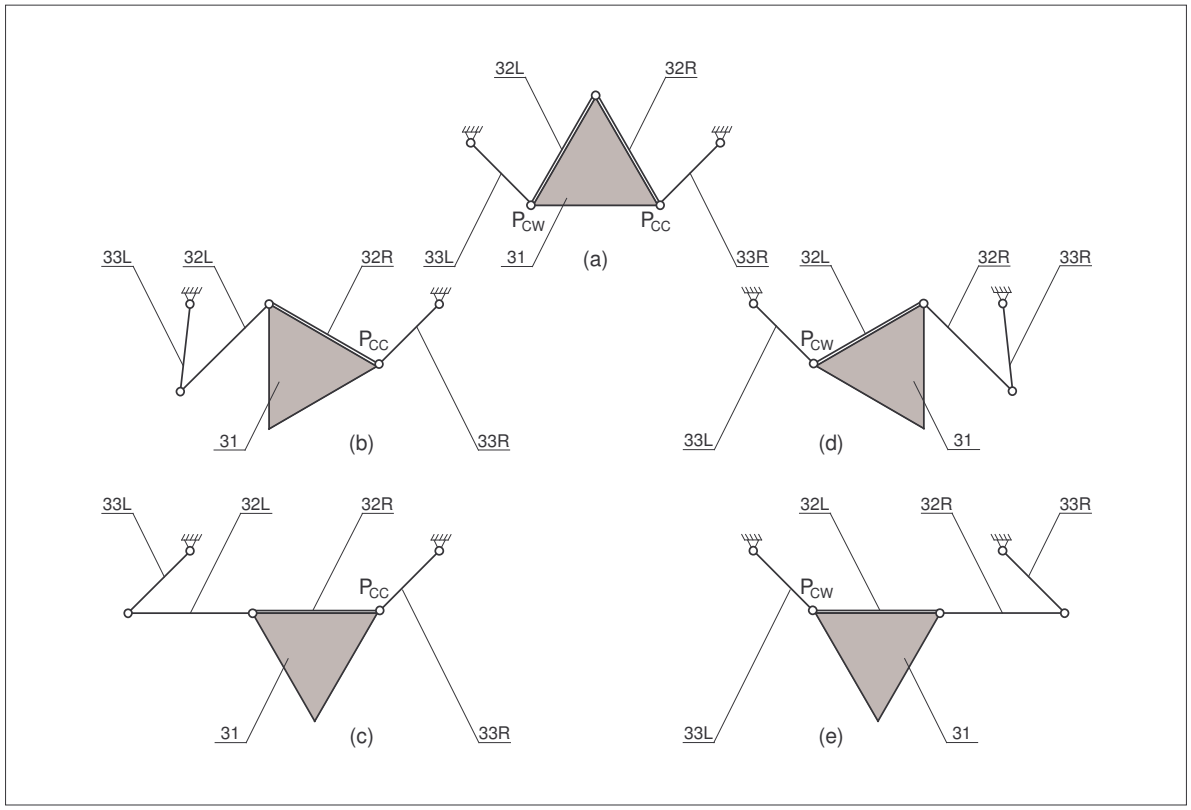

Figure 8: Operation of rocking actuation mechanism, (a) neutral position, (b) and (c) actuation of link 33L, (d) and (e) actuation of link 33R.

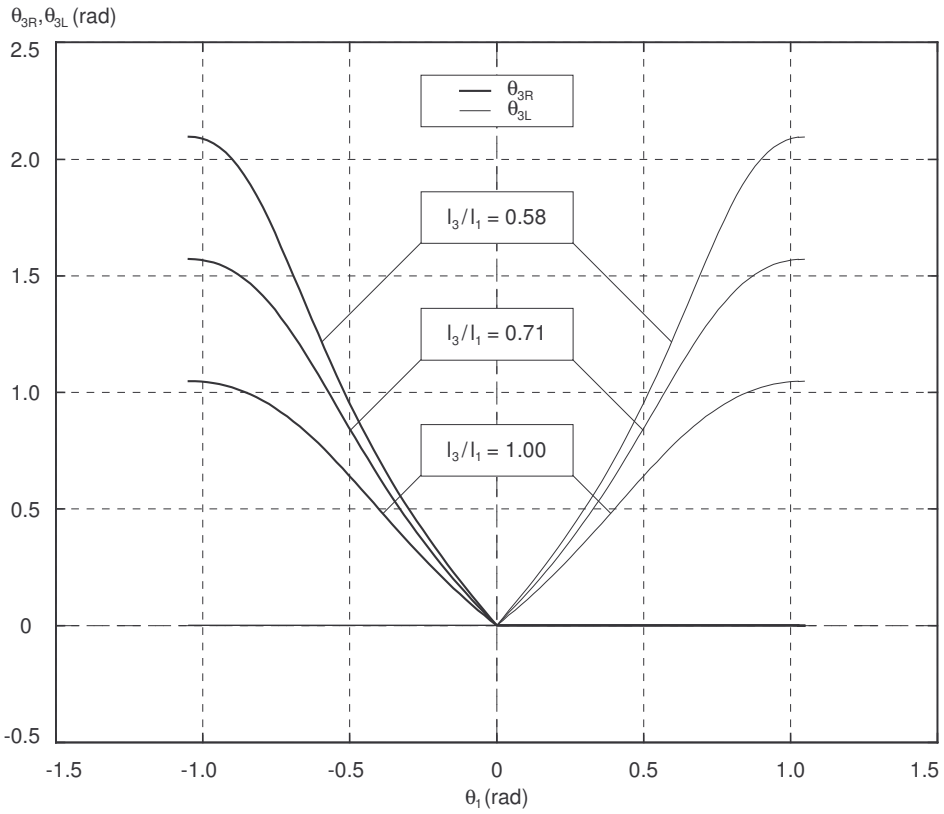

Figure 9: Kinematics of rocking actuation mechanism.

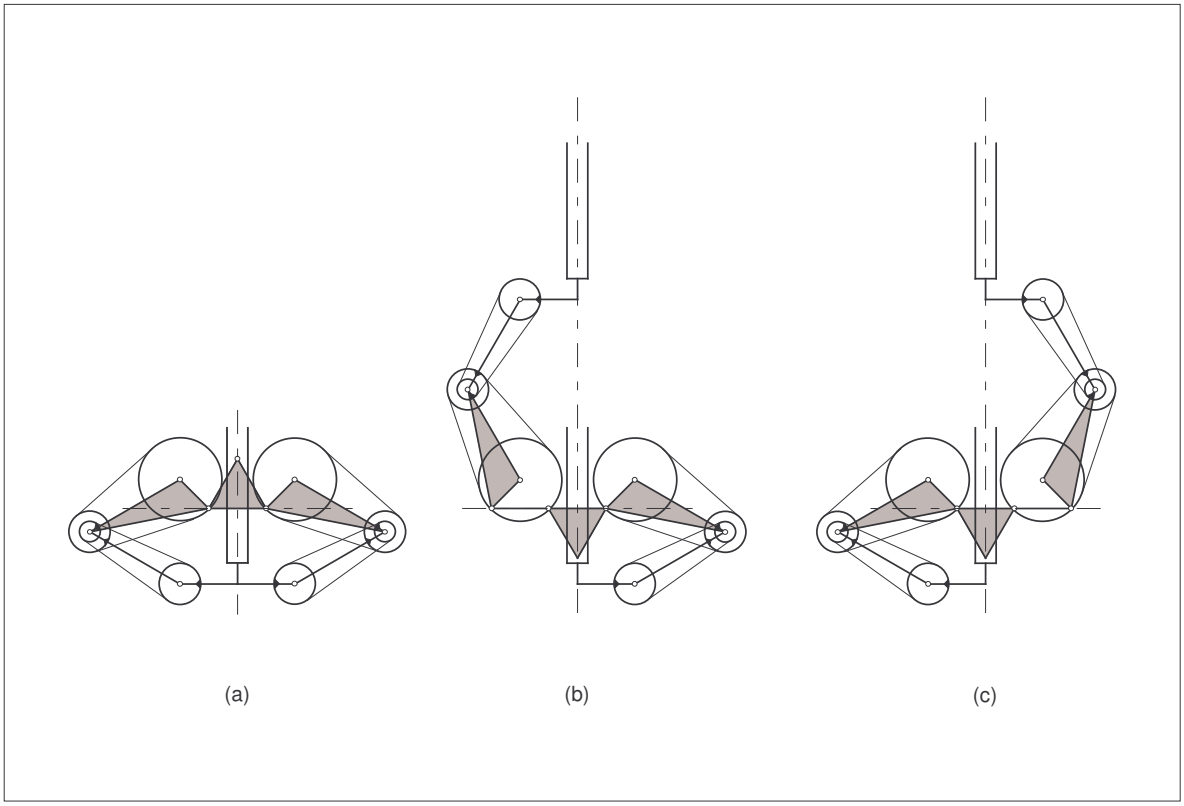

Figure 10: Dual-arm scara-type robot with rocking mechanism, (a) both arms retracted, (b) left arm extended, (c) right arm extended.

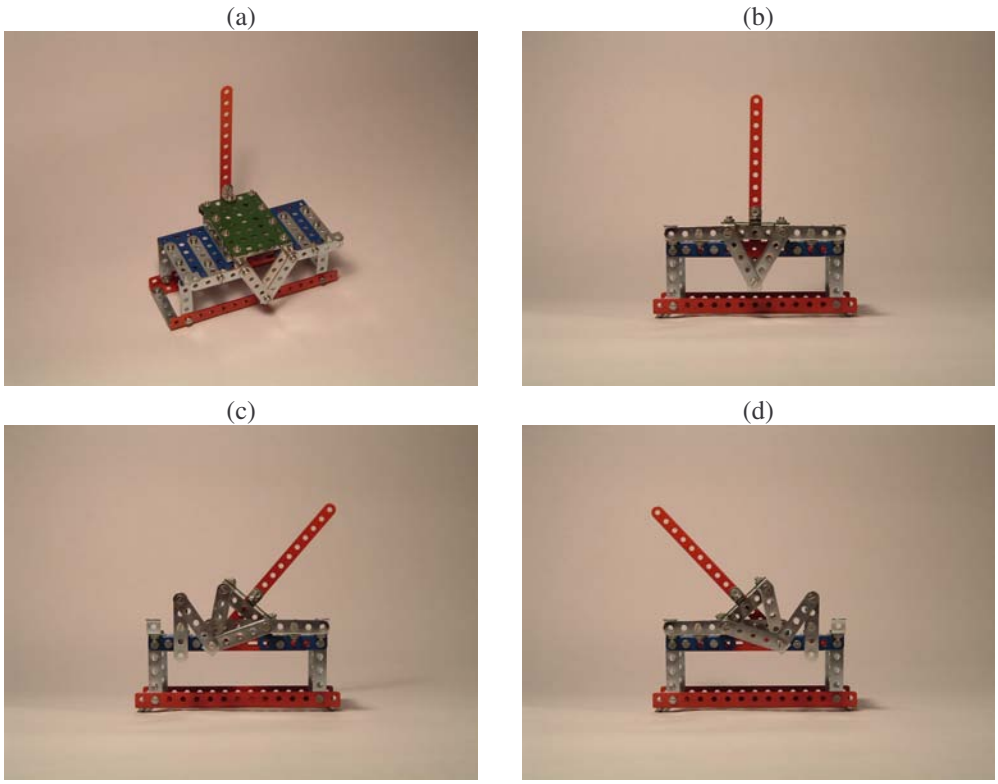

Figure 11: Model of rocking actuation mechanism, (a) overall view, (b) neutral position, (c) actuation of left branch, (d) actuation of right branch.

torque is applied to the platform 31, the link 33R rotates, while the link 33L remains stationary, as illustrated in diagrams (d) and (e).

The motion of the links 33L and 33R as a function of the angular position of the platform 31 is plotted in Figure 9. In this figure, θ_1 represents angular position of the platform 31, and θ_{3L} and θ_{3R} denote angular orientations of the links 33L and 33R, respectively. The angles θ_1, θ_{3L} and θ_{3R} are defined with respect to the initial configuration of diagram (a) of Figure 8. Note that θ_1 and θ_{3R} are considered positive in the counterclockwise direction, and θ_{3L} is taken positive in the clockwise direction. The range of motion of the links 33L and 33R can be controlled through the ratio of l_3 over l_1, where l_1 denotes the distance between the pivoting points of the platform 31 and the revolute joint which couples the links 32L and 32R to the platform 31, AE or BE, and l_3 is the length of the links 33L and 33R, EF or EG.

Applying the mechanism to the dual-arm scara-type robot of Figure 2, the links 33L and 33R are replaced by the left and right upper arms 2L and 2R of the robot, as illustrated in Figure 10. In diagram (a), the platform 31 is shown in the neutral position with both arms retracted. When torque is applied in the counterclockwise direction to the platform 31, the upper arm 2L rotates and extends the left linkage of the robot, while the upper arm 2R and the right linkage stay in the initial retracted position, as indicated in diagram (b). Similarly, when clockwise torque is applied to the platform 31, the upper arm 2R rotates and moves the right linkage, while the left upper arm 2L and the left linkage remain stationary, as illustrated in diagram (c).

A working model of an example configuration of the rocking actuation mechanism, similar but not identical to that of Figure 7, is shown in Figure 11. Photos (a) and (b) show the mechanism in its neutral position. The mechanism can be actuated manually by moving the vertical lever at the rear of the model. The left-hand-side branch of the mechanism is actuated by pushing the lever to the right, as illustrated by photo (c). Similarly, the right-hand-side branch of the mechanism moves when the lever is displaced to the left from its neutral position, as shown in photo (d).

4 DESIGN CONSIDERATIONS

The selection of the geometric properties of the rocking actuation mechanism of the previous section is relatively straightforward. Design considerations for the pivoting version of the actuation mechanism of Section 2 are discussed below.

The range of motion which is required to actuate the arm of Figure 2 depends on the retracted and extended positions of the two arm linkages, but never exceeds 180 deg. Therefore, in order to accommodate applications with different retracted and extended positions of the arm, it is convenient to design the actuation mechanism so that it provides range of motion of up to 180 deg. This design approach will be considered first.

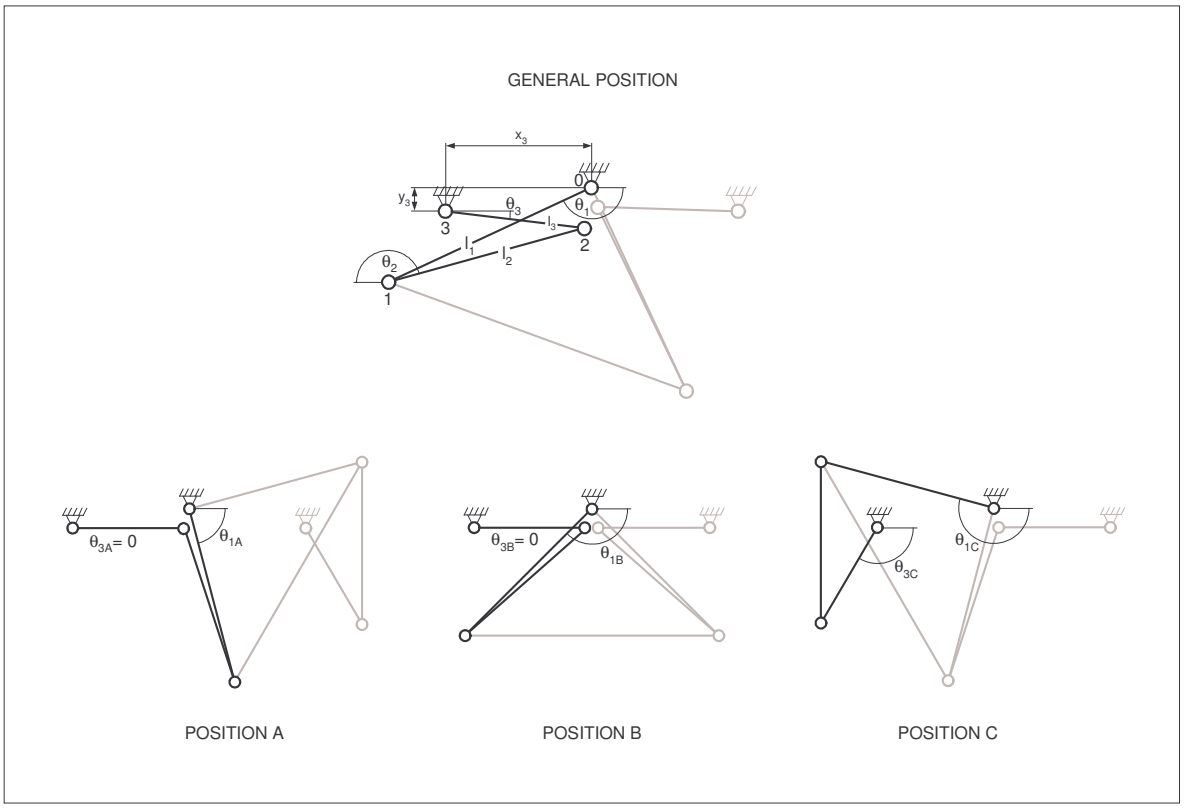

Figure 12: Design analysis of pivoting actuation mechanism.

The pivoting actuation mechanism can be conveniently represented by a pair of three-bar mechanisms, one for the left and the other for the right linkage of the arm. However, considering symmetry, one of the two three-bar mechanisms is sufficient for design analysis purposes, as illustrated in Figure 12. It is assumed that the dimensions l_1 and l_2 are specified based on the desired level of residual motion, as explained in Section 3. The designer also needs to specify the following input parameters: angular position of left/right link 1 when the right/left arm is extended, denoted as θ_{1A}; angular position of left/right link 1 when both arms are retracted, θ_{1B}; and angular position of left/right link 1 when the left/right arm is extended, θ_{1C}. These angular quantities correspond to positions A to C in Figure 12. They uniquely define the shape of the pivoting platform as well as its range of motion. The output parameters of the design process include the length of link 3, denoted as l_3, and the location of its center of rotation, x_3 and y_3.

The length of link 3 can be determined based on the following expression:

$$l_3 = \frac{\sqrt{l_2^2 - (y_{2AB} - l_1 \sin\theta_{1C})^2} - x_{2AB} - l_1 \cos\theta_{1C}}{2} \tag{1}$$

where:

$$x_{2AB} = -d_{2AB} \cos\frac{\theta_{1A} + \theta_{1B}}{2}, \quad y_{2AB} = d_{2AB} \sin\frac{\theta_{1A} + \theta_{1B}}{2} \tag{2}$$

$$d_{2AB} = \frac{l_1 \cos\frac{\theta_{1B} - \theta_{1A}}{2} - \sqrt{l_1^2\left(\cos\frac{\theta_{1B} - \theta_{1A}}{2} - 1\right)^2 + l_2^2}}{2} \tag{3}$$

Referring to Figure 12 again, the location of the center of rotation for link 3 can be calculated as follows:

$$x_3 = l_3 - d_{2AB} \cos\frac{\theta_{1A} + \theta_{1B}}{2}, \quad y_3 = d_{2AB} \sin\frac{\theta_{1A} + \theta_{1B}}{2} \tag{4}$$

As an example, the following input parameters are considered: l_1 = 1.0 m, l_2 = 0.9 m, θ_{1B} = 135 deg, $\theta_{1A} = \theta_{1B}$-90 deg, $\theta_{1C} = \theta_{1B}$+90 deg, representing a mechanism with an input range of plus/minus 90 deg. The corresponding output parameters are found as l_3 = 0.4903 m, x_3 = 0.4903 m and y_3 = 0.1503 m.

In many applications, the 180-deg output range of the actuation mechanism cannot be utilized fully because the motion of the arm is limited by constraints on the retracted and extended positions of the two arm linkages. In this case, the above design approach results in worse than optimal utilization of motor torque and position resolution. In order to achieve a solution optimized for a given range of motion of the arm, the actuation mechanism needs to be tailored to provide the corresponding output range.

For the purpose of arriving at an optimized solution, the set of input design parameters l_1, l_2, θ_{1A}, θ_{1B} and θ_{1C} needs to be augmented to specify the range of motion at the output of the

actuation mechanism. This is achieved by introducing the following additional input information: angular position of left/right link 3 when the right/left arm is extended, θ_{3A}, which is the same as when both arms are retracted, θ_{3B}; and angular position of right/left link 3 when the right/left arm is extended, θ_{3C}. These angular quantities again correspond to positions A to C in Figure 12. The output parameters of the design process remain to be the length of link 3 and the location of the center of rotation of link 3.

The length of link 3 can be determined as a solution of the following quadratic equation:

$$(a^2 + b^2)l_3^2 + 2(ad - bc)l_3 + c^2 + d^2 - l_2^2 = 0 \quad (5)$$

where:

$$a = \sin\theta_{3C} - \sin\theta_{3A}, \quad b = \cos\theta_{3C} - \cos\theta_{3A} \quad (6)$$

$$c = x_{2AB} + l_1\cos\theta_{1C}, \quad d = y_{2AB} - l_1\sin\theta_{1C} \quad (7)$$

Variables x_{2AB} and y_{2AB} are defined by Equations (2) and (3). The location of the center of rotation for link 3 then can be calculated according to these expressions:

$$x_3 = l_3\cos\theta_{3A} - d_{2AB}\cos\frac{\theta_{1A} + \theta_{1B}}{2} \quad (8)$$

$$y_3 = d_{2AB}\sin\frac{\theta_{1A} + \theta_{1B}}{2} - l_3\sin\theta_{3A} \quad (9)$$

As an example, a mechanism with an input range of plus/minus 60 deg and output range of 120 deg is designed. The following input parameters are specified: l_1 = 1.0 m, l_2 = 0.9 m, θ_{1B} = 135 deg, $\theta_{1A} = \theta_{1B}$-60 deg, $\theta_{1C} = \theta_{1B}$+60 deg, θ_{3A} = 0 deg and θ_{3C} = 120 deg. Using Equations (5) to (9), the resulting output parameters are determined as l_3 = 0.6250 m, x_3 = 0.5634 m and y_3 = 0.1063 m.

5 ALTERNATIVE CONFIGURATIONS

The mechanisms of Figures 4 and 7 represent example configurations, which a number of alternative designs with equivalent or similar functionality can be derived from. For instance, the mechanism of Figure 4 can be modified to make the links 23L and 23R rotate in the opposite direction than the platform 21 by connecting the links 22L and 22R to the platform 21 through a common revolute joint, similarly to the mechanism of Figure 7. On the flip side, the mechanism of Figure 7 can be redesigned so that the links 33L and 33R move in the same direction as the platform 31 by coupling the links 32L and 32R to the platform 31 in a non-collocated manner, similarly to the configuration depicted in Figure 4. In some applications, it may be convenient to replace rotational motion of the links 23L, 23R or 33L, 33R by sliding motion. The resulting sliding motion can be either used directly to actuate a robot or converted into rotational motion, e.g., through a rack-and-pinion or steel-band arrangement.

The use of the proposed actuation mechanisms is not limited to the dual-arm scara-type robot of Figure 2. As an example of an alternative arm arrangement, the directions in which the two linkages of the dual-arm scara-type robot extend can be offset by a given angle, e.g., 90 deg, which may be advantageous in some semiconductor manufacturing applications. In general, the concept can be extended to any robotic manipulator with multiple arms, provided that each arm is driven by a single actuator and some of the arms are never required to operate simultaneously.

6 SUMMARY

The state-of-the-art dual-arm scara-type robots utilize a pair of motors coupled to the robot mechanism through a pair of belt arrangements to control radial motion of the two arms of the robot. The alternative actuation mechanisms proposed in this paper eliminate one of the two motors, including its electronic circuitry, and replace the belt drives with rigid linkages of carefully selected geometries, thus reducing the complexity and cost, and improving the reliability and cleanliness of the robotic system.

REFERENCES

Almogy, G., Cluster Tool, U.S. Patent No. US 6,208,751 B1, March 27, 2001.

Beaulieu, D. and Pippins, M. W., Substrate Processing Apparatus Having a Substrate Transport with a Front End Extension and an Internal Substrate Buffer, U.S. Patent No. 5,882,413, March 16, 1999.

Caveney R. T. and Hofmeister C. A., Robot Handling Apparatus, U.S. Patent No. 5,765,983, June 16, 1998.

Davis J. C. and Brooks N. B., Articulated Arm Transfer Device, U.S. Patent No. 4,730,976, March 15, 1988.

Davis J. C. and Hofmeister C. A., Substrate Transport Apparatus with Dual Substrate Holders, U.S. Patent No. 5,647,724, July 15, 1997.

Garriga, R. A., Cluster Tool Architecture for Sulfur Trioxide Processing, U.S. Patent No. US 6,451,118 B1, September 17, 2002.

Hendrickson R. A., Articulated Arm Transfer Device, U.S. Patent No. 5,180,276, January 19, 1993.

Hosek M., Time-Optimum Trajectories for Robots with Multiple End-Effectors, Proceedings of 2003 ASME IMECE, November 16-21, 2003, Washington, DC.

Hosek M. and Elmali H., System of Trajectory Planning for Robotic Manipulators Based on Pre-Defined Time-Optimum Trajectory Shapes, U.S. Patent No. 6,216,058, April 10, 2001.

Hosek, M. and Elmali, H., Time Optimum Trajectory Planning for Cluster Tool Robotic Manipulators, Worldwide Automation and Performance Symposium, October 14-18, 2002, Phoenix, Arizona.

Hosek, M. and Elmali, H., Trajectory Planning and Motion Control Strategies for a Planar Three-Degree-of-Freedom Robotic Arm, U.S. Patent No. 6,643,563, November 4, 2003.

Hosek M. and Valasek M., Three-Degree-of-Freedom Parallel Robot Arm, U.S. Patent Application S/N 10/739,375, filed in 2003.

Lucas B. M., Time Optimal Trajectory for Cluster Tool Robots, U.S. Patent No. 5,655,060, August 5, 1997.

Shiraiwa H., Conveyor Apparatus, U.S. Patent No. 5,404,894, April 11,1995.